

UV-A Photocatalysis in Livestock and Poultry Farming

Subjects: Agricultural Engineering | Materials Science, Coatings & Films

Contributor: Myeongseong Lee, Jacek A. Koziel, Peiyang Li, William S. Jenks

As the scale of the livestock industry has grown with the increase in the demand for livestock and poultry products, gaseous emissions, an unwanted side effect of livestock and poultry production, are also increasing. Various mitigation technologies have been developed to reduce such air pollution, and the mitigation technologies are divided mainly into “source-based type” (meant to fundamentally reduce the emissions) and “end-of-pipe type” (physicochemical and biological treatment of the output from barns to reduce the release into the environment). Ultraviolet light (UV) can be considered as both end-of-pipe (treating exhaust air from barns) and source-based type (treating air inside the barn).

Keywords: environmental catalysis ; ultraviolet light ; air purification ; air pollution control

1. Introduction

Gaseous emissions from livestock and poultry barns include components known collectively as greenhouse gases (GHGs, e.g., CO₂), volatile organic compounds (VOC, e.g., formaldehyde), along with others not typically included in those groupings, such as hydrogen sulfide (H₂S) and ammonia (NH₃). Other noxious components of the exhausts include the particulate matter (PM) of various sizes and airborne microbes. Cumulatively, these have a detrimental effect on human health, environment, climate and quality of life in rural communities ^{[1][2][3][4][5]}.

UV treatment technology was tested in the early 2000s because of its easy application and expected mitigation effects in barns. The UV spectrum is divided into four ranges because the energy of each photon is inversely related to its wavelength; different materials absorb and react in each range. Traditionally, the ranges are known as “A” (315–400 nm), “B” (280–315 nm), “C” (200–280 nm) and “vacuum” (100–200 nm) ^[6]. The term “vacuum” arises because those wavelengths are absorbed by the components of ordinary air, and thus, the transmission of the light requires a vacuum. Although each of these causes photodamage to humans and animals on exposure, in broad terms, ultraviolet light-A (UV-A) is the least toxic, and vacuum ultraviolet (V-UV) is the most toxic. For example, UV-A is used in the commercial tanning industry, while standard germicidal bulbs are in the ultraviolet light-C (UV-C) range. In a variety of related pollutant mitigation applications, the most typical combination is the use of UV-A with a semiconductor photocatalyst that absorbs the light, causing the formation of reactive intermediates that in turn degrade the unwanted pollutants.

The photocatalysis reaction is initiated when photons of sufficient energy (more than the bandgap) are absorbed by the photocatalyst, resulting in electron (e⁻)/hole (h⁺) pair generation ^{[7][8][9][10]}. Nanosized titanium dioxide (TiO₂) is commonly applied to surfaces as a catalyst material, and it is effective with all UV with wavelengths below 400 nm ^{[7][8][11][12][13][14][15][16]}. Although the detailed mechanism of photocatalysis varies with different target pollutants, it is commonly agreed that the primary reactions responsible are interfacial redox reactions of electrons and holes with adsorbed pollutants or mediators, such as water ^{[8][17][18]}.

The applicability of UV-A photocatalytic technology to the farm has been evaluated for mitigating odorous gases and fine particulate matter concentrations, as well as for increasing the feed conversion rates ^{[19][20][21][22][23][24][25][26][27][28][29][30]}.

2. Mechanism of UV-A Photocatalysis

Nanosized titanium dioxide (TiO₂) is commonly used as a photocatalyst material due to its relatively efficient photoactivity, high stability and lowest cost in the industry ^{[7][8][11][13]}. There are TiO₂ crystalline forms of anatase, rutile and brookite, but anatase and rutile of TiO₂ are widely used commercially due to high photocatalytic activity ^{[8][12][13]}. Activation of TiO₂ is initiated at wavelengths <400 nm ^{[14][15][16]}.

Photocatalysis is, by definition, the acceleration of a photochemical reaction in the presence of a catalyst, typically, but not exclusively, with UV-A light. The primary photochemical event caused by the absorption of a photon (**Figure 1**) is the promotion of an electron from the valence band to the conduction band of the catalyst, causing charge separation, also

frequently referred to as producing a valence band “hole” (h^+) and conduction band electron (e^-) [8][9][10][12][13][17][18][31]. At its most basic level of description, holes (h^+) react with water molecules to generate hydroxyl radicals ($\cdot OH$) or oxidize organic materials through direct reaction [9]. The electrons generated in the conduction band react with molecular oxygen (O_2) to form superoxide ions ($O_2^{\cdot -}$) [9][10][13]. Although a complete description of the cascade of reactions is complex, the photon's energy is used to convert an oxidatively neutral surface to one with strong oxidizing power and modest reducing power. In the absence of water, O_2 and other substrates, the conduction band electron will collapse back to the valence band, “wasting” the absorbed energy in the form of heat release. These processes are qualitatively illustrated in **Figure 1**.

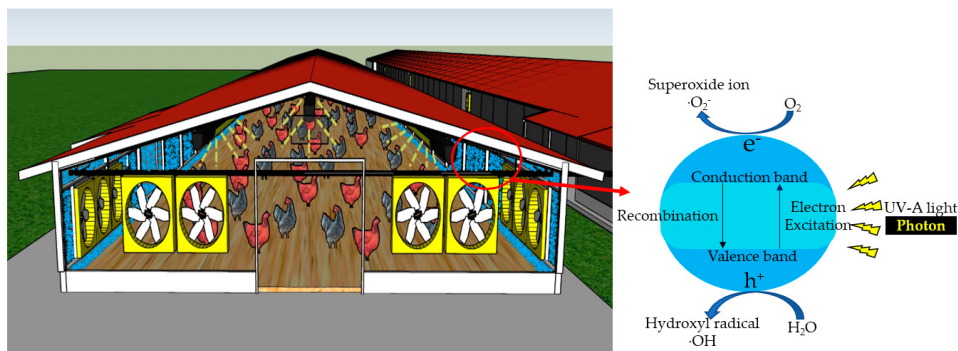


Figure 1. Mechanism of UV-A photocatalysis in livestock and poultry barns. A conceptual illustration of barn walls treated with photocatalyst (blue) irradiated with UV light (yellow rays). Note that UV-A light needs to be shielded, or the lighting duration needs to be controlled, as UV-A overexposure has side effects.

3. UV-A Photocatalysis Technology’s Effectiveness in Mitigating Targeted Air Pollutants in Livestock and Poultry Barns

3.1. Mitigation of NH_3 and H_2S

The reported mitigations of NH_3 ranged from 5 to 35% (UV-A dose: 3.9–970 $mJ\cdot cm^{-2}$, **Table 1**). Statistically significant reductions were observed from lab-scale to farm-scale studies. However, it is difficult to quantitatively evaluate the minimum UV dose and TiO_2 coating thickness required to mitigate NH_3 in real farm conditions. This is because the information on the irradiance (light intensity) and UV dose was omitted in some works [22][28] that report a relatively high mitigation rate, and the methods used for measuring light intensity were different in other reports. (As noted previously, issues of actual surface geometry could also come into play.) As implied in the Discussion, this does mean that existing data are not of sufficient quality to be able to put a universally meaningful dollar-per-gram price on pollutant removal. In addition, some inconsistencies suggest that not all variables were accounted for. For example, although significant NH_3 mitigation was reported on the pilot scale with 5.8 $mJ\cdot cm^{-2}$ of UV dose [24][26], there was no significant mitigation at the farm scale with a similar 5.3 $mJ\cdot cm^{-2}$ of UV dose [25]. It is expected that a higher UV dose is needed on the actual farm due to the harsh environmental conditions (high airborne dust and high relative humidity). Furthermore, higher UV-A doses and thicker TiO_2 coating will likely be necessary to mitigate NH_3 efficiently on the farm scale (inside the barn).

Table 1. Summary of NH_3 and H_2S percent mitigation investigated in previous studies with UV-A photocatalysis. The values reported in the table are statistically significant.

Reference	Experimental Conditions	UV-A Type (Major Wavelength)	UV Dose (Light Intensity)	Catalyst (Dose)	Gas Mitigation (Mitigation %)
[28]	Lab scale Temp: 24 °C RH: 50%	Fluorescent (365 nm)	Not reported (0.46 $mW\cdot cm^{-2}$)	TiO_2 (approx. 1 $mg\cdot cm^{-2}$)	NH_3 (35)
[20]	Lab scale (simulated poultry farm) Temp: 25 ± 3 °C RH: 12%	Fluorescent (365 nm)	<88 $mJ\cdot cm^{-2}$ (<0.44 $mW\cdot cm^{-2}$)	TiO_2 (10 $\mu g\cdot cm^{-2}$)	NH_3 (9.4) H_2S (N/S)
		LED (365 nm)	<0.97 $J\cdot cm^{-2}$ (<4.85 $mW\cdot cm^{-2}$)		NH_3 (19) H_2S (N/S)
[27]	Pilot scale (layer poultry farm) Temp: 28 ± 3 °C RH: 56%	Fluorescent (365 nm)	<75 $mJ\cdot cm^{-2}$ (<0.44 $mW\cdot cm^{-2}$)	TiO_2 (10 $\mu g\cdot cm^{-2}$)	NH_3 (5.2)
		LED (365 nm)	<0.82 $J\cdot cm^{-2}$ (<4.85 $mW\cdot cm^{-2}$)		NH_3 (8.7)

Reference	Experimental Conditions	UV-A Type (Major Wavelength)	UV Dose (Light Intensity)	Catalyst (Dose)	Gas Mitigation (Mitigation %)
[26]	Pilot scale (simulated swine farm) Temp: 11 ± 3 °C RH: $34 \pm 6\%$	LED (367 nm)	3.9 and 5.8 $\text{mJ}\cdot\text{cm}^{-2}$ ($0.41 \text{ mW}\cdot\text{cm}^{-2}$)	TiO_2 ($10 \mu\text{g}\cdot\text{cm}^{-2}$)	NH_3 (9 and 11)
[24]	Pilot scale (simulated swine farm) Temp: 19 ± 2 °C RH: $45 \pm 4\%$	LED (367 nm)	$5.8 \text{ mJ}\cdot\text{cm}^{-2}$ ($0.41 \text{ mW}\cdot\text{cm}^{-2}$)	TiO_2 ($10 \mu\text{g}\cdot\text{cm}^{-2}$)	NH_3 (6.1)
[22]	Swine farm (farrowing rooms) Temp: 24 °C (19–27) RH: 54%	Not reported (315–400 nm)	Not reported	TiO_2 ($7 \text{ mg}\cdot\text{cm}^{-2}$)	NH_3 (31)
[29]	Lab scale (simulated livestock farm) Temp: 20 ± 1 °C RH: 51%	Not reported (368 nm)	0.6 and 1.3 $\text{mJ}\cdot\text{cm}^{-2}$ ($2.3\text{--}5.6 \text{ mW}\cdot\text{cm}^{-2}$)	TiO_2 ($1.5 \text{ m}^2\cdot\text{g}^{-1}$)	H_2S (4.2 and 14)
[25]	Swine farm (finishing rooms) Temp: 29 ± 2 °C RH: $66 \pm 4\%$	LED (367 nm)	$5.3 \text{ mJ}\cdot\text{cm}^{-2}$ ($0.41 \text{ mW}\cdot\text{cm}^{-2}$)	TiO_2 ($10 \mu\text{g}\cdot\text{cm}^{-2}$)	NH_3 (N/S) H_2S (26–40)

Note: Temperature (Temp), relative humidity (RH), not significant (N/S).

The reported mitigation of H_2S ranged from 4 to 40% (UV-A dose: $0.6\text{--}5.3 \text{ mJ}\cdot\text{cm}^{-2}$). As before, it is challenging to make a direct comparison within previous research due to the differences in the TiO_2 coating thicknesses, excitation geometries and light intensity measurement. However, an important trend can be noted. In the more controlled lab-scale experiments, there was no statistically significant reduction in H_2S [20], but H_2S mitigation was observed from the more complex mixtures inevitably encountered on the farm scale. It should also be noted that H_2S oxidation via UV-A photocatalysis has been reported multiple times under “clean” laboratory conditions [32][33][34]. This state of affairs clearly needs further investigation.

3.2. Mitigation of VOCs and Odor

UV-A photocatalysis can be effective at odorous VOCs mitigation (**Table 2**). At the lab scale [29][30], some odorous VOCs were effectively removed with a relatively low UV dose compared with the pilot and farm scales. On the pilot scale [19][24][26][27], statistically significant mitigation was reported from a $1.3 \text{ mJ}\cdot\text{cm}^{-2}$ UV dose. As the UV dose increased, the VOCs mitigation effect also increased. At the farm scale [25], UV dose $\geq 2.9 \text{ mJ}\cdot\text{cm}^{-2}$ partially removed targeted VOCs, and the highest dose ($5.3 \text{ mJ}\cdot\text{cm}^{-2}$) resulted in statistically significant percent mitigation of dimethyl disulfide (62%), isobutyric acid (44%), butanoic acid (32%), *p*-cresol (40%), indole (66%) and skatole (49%). This proves that UV photocatalysis can reduce odorous VOCs even in farm environments.

Table 2. Summary of VOCs and odor percent mitigation investigated in previous studies with UV-A photocatalysis. The values reported in the table are statistically significant.

Reference	Experimental Conditions	UV-A Type (Major Wavelength)	UV Dose (Light Intensity)	Catalyst (Dose)	VOC Mitigation (Mitigation %)
[29]	Lab scale (simulated livestock farm) Temp: 20 ± 1 °C RH: 51%	Not reported (368 nm)	0.6 and 1.3 $\text{mJ}\cdot\text{cm}^{-2}$ ($2.3\text{--}5.6 \text{ mW}\cdot\text{cm}^{-2}$)	TiO_2 ($1.5 \text{ m}^2\cdot\text{g}^{-1}$)	MT (80–87) DMS (92–96) DMDS (83–91) Butan-1-ol (93–95) AA (81–89) PA (97–98) BA (98–99) VA (98–99)
[30]	Lab scale (simulated livestock farm) Temp: 40 °C R: 40%	Fluorescent (365 nm)	$12 \text{ mJ}\cdot\text{cm}^{-2}$ ($0.06 \text{ mW}\cdot\text{cm}^{-2}$)	TiO_2 ($10 \mu\text{g}\cdot\text{cm}^{-2}$)	DMDS (40) DEDS (81) DMTS (76) BA (87) Guaiacol (100) <i>p</i> -Cresol (94)

Reference	Experimental Conditions	UV-A Type (Major Wavelength)	UV Dose (Light Intensity)	Catalyst (Dose)	VOC Mitigation (Mitigation %)
[19]	Pilot scale (swine finishing room) Temp: 22–26 °C RH: 36–80%	Fluorescent (365 nm)	<1.88 mJ·cm ⁻² (<0.04 mW·cm ⁻²)	TiO ₂ (10 µg·cm ⁻²)	<i>p</i> -Cresol (22) Odor (16)
[27]	Pilot scale (layer poultry farm) Temp: 28 ± 3 °C RH: 56%	LED (365 nm)	<0.82 J·cm ⁻² (<4.85 mW·cm ⁻²)	TiO ₂ (10 µg·cm ⁻²)	DEDS (47) BA (62) <i>p</i> -Cresol (49) Skatole (35) Odor (18)
[26]	Pilot scale (simulated swine farm) Temp: 11 ± 3 °C RH: 34 ± 6%	LED (367 nm)	2.5 and 5.8 mJ·cm ⁻² (0.41 mW·cm ⁻²)	TiO ₂ (10 µg·cm ⁻²)	Butan-1-ol (19 and 41)
[24]	Pilot scale (simulated swine farm) Temp: 19 ± 2 °C RH: 45 ± 4%	LED (367 nm)	1.3 and 3.9 mJ·cm ⁻² (0.41 mW·cm ⁻²)	TiO ₂ (10 µg·cm ⁻²)	AA (N/S and 49) BA (36 and 53) <i>p</i> -Cresol (N/S and 67) Indole (N/S and 32) Odor (N/S and 58)
[25]	Swine farm (finishing rooms) Temp: 29 ± 2 °C RH: 66 ± 4%	LED (367 nm)	2.9 and 5.3 mJ·cm ⁻² (0.41 mW·cm ⁻²)	TiO ₂ (10 µg·cm ⁻²)	DMDS (22 and 62) IA (N/S and 44) BA (N/S and 32) <i>p</i> -Cresol (32 and 40) Indole (N/S and 66) Skatole (38 and 49) Odor (N/S and 40)

Note: Temperature (Temp), relative humidity (RH), methanethiol (MT), dimethyl sulfide (DMS), dimethyl disulfide (DMDS), acetic acid (AA), propionic acid (PA), butyric acid (BA), valeric acid (VA), isobutyric acid (IA), not significant (N/S).

The mitigation of odorous VOCs was consistent with the results presented for olfactory odors (16–58%). A statistically significant olfactory odor mitigation was found for higher UV doses, in which the odorous phenolic compounds were mitigated at UV doses of 3.9 mJ·cm⁻², quite comparable to the 2.9 mJ·cm⁻² dosages at which several directly targeted VOCs showed reductions on a farm scale [25].

Lee et al. [25] observed a significant change in the perceived overall odor “character” for swine barn emissions after UV-A photocatalysis. The research team described the smell of UV-A photocatalysis treated air as a mix of less-offensive “disinfectant”, “minty” or “swimming pool” scents with a weaker smell of swine manure in the background. In addition, the research team described the compound that is believed to have changed the characteristic smell as benzoic acid (or 1-octanol) based on simultaneous chemical and sensory analysis of the GS-MS olfactory test. Although further research on odor character change is still needed, it is interesting that it is the first study to track odor character change after UV-A photocatalysis.

It is important to underline the generation of some targeted compounds for all UV doses in the previous studies [25]. The generated compounds (several in the VFAs group, DMDS and phenol) are odorants that are considered slightly less impactful than *p*-cresol, skatole and indole (representative phenolic compounds), and the generated compounds appear to be partial degradation products from compounds known to be in the original mixtures. Therefore, it is feasible to hypothesize that the generated compounds offset the overall odor mitigation.

3.3. Mitigation of GHGs

For the GHGs (Table 3), the previous lab- and pilot-scale study did not find significant mitigation in CH₄ under UV-A photocatalysis; however, moderate mitigations (15–27%) were observed with the farm scale and high TiO₂ coating thickness [21][22]. It is widely understood from closely related research in photocatalysis in both air and water that hydrocarbons are indeed oxidized (ultimately to CO₂) by TiO₂ [35][36]; the lack of mitigation in the lab- and pilot-scale reports may reflect insufficient mass transport or other competitive reactions that stop the expected reduction in methane levels. There is little doubt that, in principle, methane should be oxidized.

Table 3. Summary of GHGs percent mitigation investigated in previous studies with UV-A photocatalysis. The values reported in the table are statistically significant.

Reference	Experimental Conditions	UV-A Type (Major Wavelength)	UV Dose (Light Intensity)	Catalyst (Dose)	GHGs Mitigation (Mitigation %)
[20]	Lab scale (simulated poultry farm) Temp: 25 ± 3 °C RH: 12%	Fluorescent (365 nm)	<88 mJ·cm ⁻² (<0.44 mW·cm ⁻²)	TiO ₂ (10 µg·cm ⁻²)	N ₂ O (3.3)
		LED (365 nm)	<0.97 J·cm ⁻² (<4.85 mW·cm ⁻²)		CO ₂ (3.8) N ₂ O (10)
[19]	Pilot scale (swine finishing room) Temp: 22–26 °C RH: 36–80%	Fluorescent (365 nm)	<1.88 mJ·cm ⁻² (<0.04 mW·cm ⁻²)	TiO ₂ (10 µg·cm ⁻²)	CO ₂ (–3.1) N ₂ O (8.7)
[27]	Pilot scale (layer poultry farm) Temp: 28 ± 3 °C RH: 56%	Fluorescent (365 nm)	<75 mJ·cm ⁻² (<0.44 mW·cm ⁻²)	TiO ₂ (10 µg·cm ⁻²)	N ₂ O (7.5)
		LED (365 nm)	<0.82 J·cm ⁻² (<4.85 mW·cm ⁻²)		N ₂ O (13)
[24]	Pilot scale (simulated swine farm) Temp: 19 ± 2 °C RH: 45 ± 4%	LED (367 nm)	2.5 and 3.9 mJ·cm ⁻² (0.41 mW·cm ⁻²)	TiO ₂ (10 µg·cm ⁻²)	N ₂ O (9.0 and 4.3) CO ₂ (N/S and –25.8)
[25]	Swine farm (finishing rooms) Temp: 29 ± 2 °C RH: 66 ± 4%	LED (367 nm)	2.9 and 5.3 mJ·cm ⁻² (0.41 mW·cm ⁻²)	TiO ₂ (10 µg·cm ⁻²)	N ₂ O (9.4 and 12) CO ₂ (–33.7 and –27.8)
[22]	Swine farm (farrowing rooms) Temp: 24 °C (19–27) RH: 54%	Not reported (315–400 nm)	Not reported	TiO ₂ (7 mg·cm ⁻²)	CH ₄ (15) CO ₂ (11) N ₂ O (4.2)
[21]	Swine farm (weaning rooms) Temp: 26 °C (24–30) RH: 56% (52–90)	Not reported (315–400 nm)	Not reported	TiO ₂ (7 mg·cm ⁻²)	CH ₄ (27)

Note: Temperature (Temp), relative humidity (RH), not significant (N/S).

A surprising slight decrease in CO₂ was reported in a few previous studies [20][22], but most research has reported an increase in CO₂ concentration after UV-A photocatalysis [19][23][24][25][27]. In general, CO₂ is the oxidative endpoint for photocatalytic oxidation of virtually all carbon-containing compounds under conditions like those used here. Thus, its mitigation would not derive from its chemical removal [20][27].

N₂O was mitigated by 3–13% under UV-A photocatalysis with 1.9 mJ·cm⁻² or higher doses [19][20][22][23][24][25][26][27]. For N₂O concentration, mitigation continuously appeared at a low rate, but the mitigation efficiency did not always increase as the UV dose increased.

In general, N₂O and O₃ are known not to absorb significantly in the UV-A range, meaning that they are not subject to direct photolytic degradation at these wavelengths. However, indirect effects through more complex reaction paths can certainly affect their observed concentrations. N₂O might be reduced by the reaction of the hydroxyl radical and activated O₃.

3.4. Mitigation of Pollutants

Table 4 summarized the additional UV-A photocatalysis mitigation effects other than the gases previously listed.

Table 4. Summary of mitigation effects in previous studies with UV-A photocatalysis. The values reported in the table are statistically significant.

Reference	Experimental Conditions	UV-A Type (Major Wavelength)	UV Dose (Light Intensity)	Catalyst (Dose)	Mitigation (Mitigation %)
[20]	Lab scale (simulated poultry farm) Temp: 25 ± 3 °C RH: 12%	Fluorescent (365 nm)	<88 mJ·cm ⁻² (<0.44 mW·cm ⁻²)	TiO ₂ (10 µg·cm ⁻²)	O ₃ (24)
		LED (365 nm)	<0.97 J·cm ⁻² (<4.85 mW·cm ⁻²)		O ₃ (48)

Reference	Experimental Conditions	UV-A Type (Major Wavelength)	UV Dose (Light Intensity)	Catalyst (Dose)	Mitigation (Mitigation %)
[24]	Pilot scale (simulated swine farm) Temp: 19 ± 2 °C RH: $45 \pm 4\%$	LED (367 nm)	1.3 and $5.8 \text{ mJ}\cdot\text{cm}^{-2}$ ($0.41 \text{ mW}\cdot\text{cm}^{-2}$)	TiO ₂ ($10 \mu\text{g}\cdot\text{cm}^{-2}$)	O ₃ (100 and 100)
[27]	Pilot scale (layer poultry farm) Temp: 28 ± 3 °C RH: 56%	Fluorescent (365 nm)	$<75 \text{ mJ}\cdot\text{cm}^{-2}$ ($<0.44 \text{ mW}\cdot\text{cm}^{-2}$)	TiO ₂ ($10 \mu\text{g}\cdot\text{cm}^{-2}$)	O ₃ (100)
		LED (365 nm)	$<0.82 \text{ J}\cdot\text{cm}^{-2}$ ($<4.85 \text{ mW}\cdot\text{cm}^{-2}$)		O ₃ (100)
[21]	Swine farm (weaning rooms) Temp: 26 °C (24–30) RH: 56% (52–90)	Not reported (315–400 nm)	Not reported	TiO ₂ ($7 \text{ mg}\cdot\text{cm}^{-2}$)	PM 10 (17) FCR (–12)
[25]	Swine farm (finishing rooms) Temp: 29 ± 2 °C RH: $66 \pm 4\%$	LED (367 nm)	$5.3 \text{ mJ}\cdot\text{cm}^{-2}$ ($0.41 \text{ mW}\cdot\text{cm}^{-2}$)	TiO ₂ ($10 \mu\text{g}\cdot\text{cm}^{-2}$)	O ₃ (100)
[23]	Swine farm (finishing rooms) Temp: 29 ± 2 °C RH: $66 \pm 4\%$	LED (367 nm)	$5.3 \text{ mJ}\cdot\text{cm}^{-2}$ ($0.41 \text{ mW}\cdot\text{cm}^{-2}$)	TiO ₂ ($10 \mu\text{g}\cdot\text{cm}^{-2}$)	CFU (49–51) PM (N/S)

Note: Temperature (Temp), relative humidity (RH), particular matter (PM), feed conversion ratio (FCR), colony-forming unit (CFU), not significant (N/S).

Ozone (O₃) is an interesting case because of its well-known atmospheric role in protecting the surface of the earth from UV irradiation. However, O₃ does not absorb the light of wavelengths > 290 nm (i.e., UV-A), so its direct photochemistry is not involved in the reported mitigation using UV-A irradiation. Instead, either a reaction with the catalyst or ordinary indirect photocatalytic reactions must be involved [37]. O₃ has been reported to increase the reduction in target gas during photocatalysis [38][39][40][41] because O₃ could be reduced to ozonide radicals (O₃[•]). In this instance, O₃ would be an electron sink (in parallel with ambient O₂), but the resulting ozonide is sufficiently reactive that the ozone is destroyed rather than reformed by oxidation.

At both farm and pilot scales, ambient O₃ was removed completely, whereas at the lab scale, mitigation was significant but not complete (24–48%). It is reasonable to speculate that a wider variety of compounds are produced in the larger-scale reactions than in the “controlled” lab reactions and that some of these are reactive with ozone or ozonide.

The effects of UV-A photocatalysis on PM have been investigated by two groups. An Italian research team [21] reported that UV-A photocatalysis with TiO₂ mitigated airborne PM 10, which is a PM with diameters that are usually 10 microns or less (17%) inside a ~390 head nursery barn, while also improving feed conversion efficiency (12%). The mechanism of PM mitigation was not reported and was unclear; thus, the Iowa (USA) research team independently investigated the PM mitigation effect. No statistically significant PM mitigation was reported in experiments that used different minimum efficiency reporting values (MERV) rating filters to create three different airborne PM concentration levels [23].

Although pathogens are obviously much larger than individual gas molecules, it is well known in other applications of photocatalytic methods that they can be inactivated without the need for complete chemical degradation. The research of Rodriguez-Silva et al. [42] is an example of microorganism inactivation in liquid water. The previous precedent showed that microbe deactivation by photocatalysis is sensitive to catalyst loading and UV dose, like chemical degradation. Therefore, it is considered that there is a potential to inactivate airborne microorganisms if appropriate UV-A dose and TiO₂ coating are satisfied. Indeed, UV-A photocatalysis treatment was reported to mitigate airborne microbial colony-forming units (CFUs, a measure of the airborne microbial load) by 15–95% [23]. Normalization of the measured airborne pathogen concentrations by smaller PM size concentrations led to the significant mitigation (49–51%, p -value < 0.03) effect of UV-A photocatalysis on pathogen inactivation [23].

References

- Buijsman, E.; Erisman, J.-W. Wet deposition of ammonium in Europe. *J. Atmos. Chem.* 1988, 6, 265–280.
- Casey, J.A.; Kim, B.F.; Larsen, J.; Price, L.B.; Nachman, K.E. Industrial food animal production and community health. *Curr. Environ. Health Rep.* 2015, 2, 259–271.

3. Herrero, M.; Gerber, P.; Vellinga, T.; Garnett, T.; Leip, A.; Opio, C.; Westhoek, H.; Thornton, P.K.; Olesen, J.; Hutchings, N. Livestock and greenhouse gas emissions: The importance of getting the numbers right. *Anim. Feed. Sci. Technol.* 2011, 166, 779–782.
4. Rappert, S.; Müller, R. Odor compounds in waste gas emissions from agricultural operations and food industries. *Waste Manag.* 2005, 25, 887–907.
5. Schiffman, S.S. Livestock odors: Implications for human health and well-being. *J. Anim. Sci.* 1998, 76, 1343–1355.
6. Bolton, J.R.; Cotton, C.A. *The Ultraviolet Disinfection Handbook*; American Water Works Association: Denver, CO, USA, 2011.
7. Hashimoto, K.; Irie, H.; Fujishima, A. TiO₂ photocatalysis: A historical overview and future prospects. *Jpn. J. Appl. Phys.* 2005, 44, 8269.
8. Schneider, J.; Matsuoka, M.; Takeuchi, M.; Zhang, J.; Horiuchi, Y.; Anpo, M.; Bahnemann, D.W. Understanding TiO₂ photocatalysis: Mechanisms and materials. *Chem. Rev.* 2014, 114, 9919–9986.
9. Haque, M.M.; Bahnemann, D.; Muneer, M. Photocatalytic degradation of organic pollutants: Mechanisms and kinetics. In *Organic Pollutants Ten Years after the Stockholm Convention—Environmental and Analytical Update*; IntechOpen: London, UK, 2012; p. 293.
10. Vautier, M.; Guillard, C.; Herrmann, J.-M. Photocatalytic degradation of dyes in water: Case study of indigo and of indigo carmine. *J. Catal.* 2001, 201, 46–59.
11. Zaleska, A. Doped-TiO₂: A review. *Recent Pat. Eng.* 2008, 2, 157–164.
12. Athanasekou, C.P.; Moustakas, N.G.; Morales-Torres, S.; Pastrana-Martínez, L.M.; Figueiredo, J.L.; Faria, J.L.; Silva, A.M.; Dona-Rodríguez, J.M.; Romanos, G.E.; Falaras, P. Ceramic photocatalytic membranes for water filtration under UV and visible light. *Appl. Catal. B Environ.* 2015, 178, 12–19.
13. Lee, H.J.; Park, Y.G.; Lee, S.H.; Park, J.H. Photocatalytic properties of TiO₂ according to manufacturing method. *Korean Chem. Eng. Res.* 2018, 56, 156–161.
14. Chong, M.N.; Jin, B.; Chow, C.W.; Saint, C. Recent developments in photocatalytic water treatment technology: A review. *Water Res.* 2010, 44, 2997–3027.
15. Gomes, J.F.; Leal, I.; Bednarczyk, K.; Gmurek, M.; Stelmachowski, M.; Zaleska-Medynska, A.; Quinta-Ferreira, M.E.; Costa, R.; Quinta-Ferreira, R.M.; Martins, R.C. Detoxification of parabens using UV-A enhanced by noble metals—TiO₂ supported catalysts. *J. Environ. Chem. Eng.* 2017, 5, 3065–3074.
16. Jia, J.; Li, D.; Wan, J.; Yu, X. Characterization and mechanism analysis of graphite/C-doped TiO₂ composite for enhanced photocatalytic performance. *J. Ind. Eng. Chem.* 2016, 33, 162–169.
17. Abe, R. Recent progress on photocatalytic and photoelectrochemical water splitting under visible light irradiation. *J. Photochem. Photobiol. C Photochem. Rev.* 2010, 11, 179–209.
18. Maeda, K.; Domen, K. Photocatalytic water splitting: Recent progress and future challenges. *J. Phys. Chem. Lett.* 2010, 1, 2655–2661.
19. Maurer, D.L.; Koziel, J.A. On-farm pilot-scale testing of black ultraviolet light and photocatalytic coating for mitigation of odor, odorous VOCs, and greenhouse gases. *Chemosphere* 2019, 221, 778–784.
20. Lee, M.; Wi, J.; Koziel, J.A.; Ahn, H.; Li, P.; Chen, B.; Meir Khanuly, Z.; Banik, C.; Jenks, W. Effects of UV-A Light Treatment on Ammonia, hydrogen sulfide, greenhouse gases, and ozone in simulated poultry barn conditions. *Atmosphere* 2020, 11, 283.
21. Costa, A.; Chiarello, G.L.; Selli, E.; Guarino, M. Effects of TiO₂ based photocatalytic paint on concentrations and emissions of pollutants and on animal performance in a swine weaning unit. *J. Environ. Manag.* 2012, 96, 86–90.
22. Guarino, M.; Costa, A.; Porro, M. Photocatalytic TiO₂ coating—To reduce ammonia and greenhouse gases concentration and emission from animal husbandries. *Bioresour. Technol.* 2008, 99, 2650–2658.
23. Lee, M.; Koziel, J.A.; Macedo, N.R.; Li, P.; Chen, B.; Jenks, W.S.; Zimmerman, J.; Paris, R.V. Mitigation of particulate matter and airborne pathogens in swine barn emissions with filtration and UV-A photocatalysis. *Catalysts* 2021, 11, 1302.
24. Lee, M.; Koziel, J.A.; Murphy, W.; Jenks, W.S.; Chen, B.; Li, P.; Banik, C. Evaluation of TiO₂ based photocatalytic treatment of odor and gaseous emissions from swine manure with UV-A and UV-C. *Animals* 2021, 11, 1289.
25. Lee, M.; Koziel, J.A.; Murphy, W.; Jenks, W.S.; Chen, B.; Li, P.; Banik, C. Mitigation of odor and gaseous emissions from swine barn with UV-A and UV-C photocatalysis. *Atmosphere* 2021, 12, 585.
26. Lee, M.; Koziel, J.A.; Murphy, W.; Jenks, W.S.; Fonken, B.; Storjohann, R.; Chen, B.; Li, P.; Banik, C.; Wahe, L. Design and testing of mobile laboratory for mitigation of gaseous emissions from livestock agriculture with photocatalysis. *Int.*

27. Lee, M.; Li, P.; Koziel, J.A.; Ahn, H.; Wi, J.; Chen, B.; Meirikhany, Z.; Banik, C.; Jenks, W.S. Pilot-scale testing of UV-A light treatment for mitigation of NH₃, H₂S, GHGs, VOCs, odor, and O₃ inside the poultry barn. *Front. Chem.* 2020, 8, 613.
28. Wu, H.; Ma, J.; Li, Y.; Zhang, C.; He, H. Photocatalytic oxidation of gaseous ammonia over fluorinated TiO₂ with exposed (0 0 1) facets. *Appl. Catal. B Environ.* 2014, 152, 82–87.
29. Yao, H.; Feilberg, A. Characterisation of photocatalytic degradation of odorous compounds associated with livestock facilities by means of PTR-MS. *Chem. Eng. J.* 2015, 277, 341–351.
30. Zhu, W.; Koziel, J.A.; Maurer, D.L. Mitigation of livestock odors using black light and a new titanium dioxide-based catalyst: Proof-of-concept. *Atmosphere* 2017, 8, 103.
31. Linsebigler, A.L.; Lu, G.; Yates, J.T., Jr. Photocatalysis on TiO₂ surfaces: Principles, mechanisms, and selected results. *Chem. Rev.* 1995, 95, 735–758.
32. Alonso-Tellez, A.; Robert, D.; Keller, N.; Keller, V. A parametric study of the UV-A photocatalytic oxidation of H₂S over TiO₂. *Appl. Catal. B Environ.* 2012, 115, 209–218.
33. Portela, R.; Canela, M.C.; Sánchez, B.; Marques, F.C.; Stumbo, A.M.; Tessinari, R.F.; Coronado, J.M.; Suárez, S. H₂S photodegradation by TiO₂/M-MCM-41 (M= Cr or Ce): Deactivation and by-product generation under UV-A and visible light. *Appl. Catal. B Environ.* 2008, 84, 643–650.
34. Brancher, M.; Franco, D.; de Melo Lisboa, H. Photocatalytic oxidation of H₂S in the gas phase over TiO₂-coated glass fiber filter. *Environ. Technol.* 2016, 37, 2852–2864.
35. Yuliaty, L.; Yoshida, H. Photocatalytic conversion of methane. *Chem. Soc. Rev.* 2008, 37, 1592–1602.
36. Cybula, A.; Klein, M.; Zaleska, A. Methane formation over TiO₂-based photocatalysts: Reaction pathways. *Appl. Catal. B Environ.* 2015, 164, 433–442.
37. Ohtani, B.; Zhang, S.-W.; Nishimoto, S.-I.; Kagiya, T. Catalytic and photocatalytic decomposition of ozone at room temperature over titanium (IV) oxide. *J. Chem. Soc. Faraday Trans.* 1992, 88, 1049–1053.
38. Černigoj, U.; Štangar, U.L.; Trebše, P. Degradation of neonicotinoid insecticides by different advanced oxidation processes and studying the effect of ozone on TiO₂ photocatalysis. *Appl. Catal. B Environ.* 2007, 75, 229–238.
39. Hernández-Alonso, M.a.D.; Coronado, J.M.; Maira, A.J.; Soria, J.; Loddo, V.; Augugliaro, V. Ozone enhanced activity of aqueous titanium dioxide suspensions for photocatalytic oxidation of free cyanide ions. *Appl. Catal. B Environ.* 2002, 39, 257–267.
40. Pichat, P.; Cermenati, L.; Albin, A.; Mas, D.; Delprat, H.; Guillard, C. Degradation processes of organic compounds over UV-irradiated TiO₂. Effect of ozone. *Res. Chem. Intermed.* 2000, 26, 161–170.
41. Pichat, P.; Disdier, J.; Hoang-Van, C.; Mas, D.; Goutailler, G.; Gaysse, C. Purification/deodorization of indoor air and gaseous effluents by TiO₂ photocatalysis. *Catal. Today* 2000, 63, 363–369.
42. Rodrigues-Silva, C.; Miranda, S.M.; Lopes, F.V.; Silva, M.; Dezotti, M.; Silva, A.M.; Faria, J.L.; Boaventura, R.A.; Vilar, V.J.; Pinto, E. Bacteria and fungi inactivation by photocatalysis under UVA irradiation: Liquid and gas phase. *Environ. Sci. Pollut. Res.* 2017, 24, 6372–6381.